Heliyon 9 (2023) e12687

Contents lists available at ScienceDirect

Heliyon

journal homepage: www.cell.com/heliyon

Research article

Treatment of tannery effluent by adsorption onto fly ash released from thermal power stations: Characterisation, optimization, kinetics, and isotherms

Karima Elkarrach [a,*], Anass Omor [b], Fatima Atia [a], Omar Laidi [a], Mohamed Benlemlih [a], Mohammed Merzouki [a]

[a] *Laboratory of Biotechnology, Environment, Agri-food, and Health, Faculty of Sciences Dhar El Mahraz, Sidi Mohamed Ben Abdallah University, Fez, Morocco*

[b] *Laboratory of Electrochemistry Engineering, Modeling and Environment. Faculty of Sciences Dhar El Mahraz, University of Sidi Mohamed Ben Abdallah, Fez, Morocco*

ARTICLE INFO

Keywords:
Tannery effluent
Fly ash
Characterisation
Adsorption
kinetics
isotherms

ABSTRACT

Fly ash is a significant pollutant in thermal power stations. Although this waste harms the environment and humans, it is badly removed and managed, and only a few studies are interested in this waste. For that, this study aims to valorise fly ash into potential adsorbents to treat tannery effluents for the first time. The physicochemical characterisation showed that fly ash has a pHpzc of 9.78, a very porous structure, a high specific surface area of 3127.2 m^2/g with a total pore volume of 3.27 cm^3/g, and a high silica and aluminium percentage. SEM showed that the fly ash studied has a small particle size ranging between 32 nm and 100 μm. Batch adsorption experiments were done, and the effects of adsorption parameters were investigated. The kinetics and isotherms models indicate that the equilibriums were achieved in 30 min, where the maximum uptake capacity was 2496, 223.7 and 106.8 mg/g for Chemical Oxygen Demand (COD), chromium (VI) and sulfide ions, respectively. The kinetic data were well fitted to the pseudo-second-order model and showed that adsorption onto fly ash may be chemical and physical simultaneously. Freundlich's model gave a better fit for the experimental adsorption equilibrium data and displayed multilayer adsorption. The thermodynamic isotherm showed that the adsorption onto fly ash is thermodynamically spontaneous ($\Delta G^\circ < 0$) and endothermic ($\Delta H^\circ > 0$). In conclusion, fly ash, which is a free material, has a more robust adsorption capacity than other expensive materials. Thus, it can be a promising, eco-friendly, attractive adsorbent for industrial wastewater treatment.

1. Introduction

Tannery effluents have been wordily classed as the most toxic effluent due to the high amount of chromium, sulfide and hard non-biodegradable matter [1]. Thus, treating these effluents before their release into the environment is mandatory. In this regard, many biological and physicochemical processes have been studied for the treatment of these tannery wastewaters, such as sequencing batch reactor [2], bio-augmentation [3], chemical precipitation [4], oxidation [5], electro-coagulation [6], adsorption [7], chemical

* Corresponding author.
E-mail address: karima-elkarrach@outlook.com (K. Elkarrach).

https://doi.org/10.1016/j.heliyon.2022.e12687
Received 20 August 2022; Received in revised form 16 December 2022; Accepted 21 December 2022
Available online 4 January 2023

precipitation coupled to the sequencing batch reactor coupled [8] … etc. However, because of their complexity, all these technologies could not remove the entire pollution from these effluents. In addition, some processes generate other pollution, namely coagulation-flocculation, which increases the conductivity and the turbidity, electro-coagulation, produces a high amount of sludge, and bio-augmentation focuses on one specific pollutant, etc.

Adsorption is widely known as an emerging, straightforward and promising technology for treating industrial sewage and tannery effluent in particular. This process is based on the retention of pollutants by an adsorbent, of which commercial activated carbon is considered the most efficient. However, it is still the most expensive as well. Therefore, this technique will be more attractive if a low-cost and efficient material is founded. For that, many low adsorbents have been studied; those materials were inorganic or biological such as sand [9], eggshell [10], clays [11], wood [12], rice husk [13], tea waste [14], cement dust [15] … etc. The quality and efficiency of those materials may be enhanced by their activation, which can be done using thermal or chemical processes, or even both. Nevertheless, the activation may increase the costs of the adsorption process. Furthermore, all those low-cost adsorbents studied could not remove the entire pollution from these tannery effluents, or satisfy the standards of discharge in terms of chromium, COD and sulfide. Hence, it will be promising to find a new low adsorbent more efficient for the treatment of these toxic effluents.

In Morocco, thermal power plants use coal to produce electricity, in which the coal combustion results in a large quantity of ash. This amount is estimated to be around 600,000 tons, where 80% is fly ash [16]. This considerable amount of fly ash is released directly into the atmosphere and causes many health and environmental problems. Thus, removing this waste is essential, and its valorisation will be very interesting. Some studies have shown fly ash's effectiveness and its high uptake potential for the treatment of textile effluents [17]. Otherwise, the characteristic of this fly ash varies considerably among studies and countries due to many factors such as coal composition and thermal process of combustion [16]. Moreover, there is no study on the removal of COD, chromium, and sulfide from real tannery effluent by adsorption onto fly ash.

Considering all the above, the main objective of this present study is to investigate the potential adsorption capacity of Moroccan fly ash for the treatment of real tannery effluent. The second objective was the study of adsorption behavior by performing the kinetic, isotherm and thermodynamic models.

2. Materials and methods

2.1. Tannery effluent

The composite tannery effluent was collected from a modern tanning industry in Fez city, Morocco. The sampling and its conservation were done according to the methods described by Rodier [18]. Table 1, shows the physicochemical characteristics of this composite effluent.

2.2. Fly ash characterisation

2.2.1. Sampling

The fly ash was collected from the JLEC industry in Jorf Lasfar, El Jadida, Morocco. After coal combustion, the fly ash was released, captured through electrostatic precipitators, and then stored in silos, wherein the sampling was done.

Fig. 1 demonstrates the macroscopic appearance of this waste. Generally, it has a grey color and excellent granules like cement. Under the optic microscope, it has brilliant grains with more or less spherical shapes.

2.2.2. Iodine number

The iodine number was carried out according to the standard method ASTM D4607-86 [21]. The procedure is as follows: a mass of 0.05 g of fly ash was placed in an Erlenmeyer of 250 mL, and then, 10 mL of dilute HCl (5% by weight) was added. Then, 100 mL of iodine solution (0.1 N) was added to the vigorously shaken mixture for 30 min. After filtration, 50 mL of the filtrate was titrated with sodium thiosulfate solution (0.1 M). The iodine number has expressed in mg/g.

2.2.3. PH at the point of zero charge

The pH at the point of zero charges (pHpzc) was determined according to the standard method described by Furlan [22]. In a series of 250 mL flasks, 50 mL of NaCl solution (0.1 M) was taken, and its pH was adjusted in a range of 2–12 (with intervals of 2) using HCl and NaOH solutions (0.1 M). After that, 0.05 g of adsorbent was added to each flask, and then the mixture was shaken for 48 h. Further, pH is measured, and the point of zero charges is determined by plotting ΔpH (pH initial− pH final) against pH initial.

Table 1
Results of the physicochemical parameters of composite tannery effluent of Fez city in Morocco [19].

Parameters	Average values	Moroccan Standards [20]
pH	9 ± 0.2	5.5–8.5
COD (mg O_2/L)	14,500 ± 250	500
S^{2-} (mg/L)	410.6 ± 12.4	1
Total Cr (mg/L)	920.04 ± 0.45	2
Cr(VI) (mg/L)	390.08 ± 0.8	0.5

Fig. 1. Macroscopic aspect of fly ash collected from JLEC Company ELjadida, Morocco.

2.2.4. Specific surface area

The total surface area, the size and volume of pores were performed to assess the surface characteristics. They were determined by nitrogen adsorption isotherms at 77 K at different partial pressures, using a surface area and pore size analyzer (ASAP-2000 Micrometrics), and according to the Brunauer Emmett and Teller (BET) equation [23]. The size and volume of pores were obtained by Barret-Joyner-Halenda (BJH) method using the desorption branch. The Horvath-Kawazoe (HK) and the Barrett-Joyner-Halenda (BJH) methods were adopted to define the micropore and mesoporous volumes, respectively. The average pore diameter was calculated from the BET surface area (S_{BET}) and total pore volume (VT). This analysis was done at Industrial Engineering Department at Padova University-Italy.

2.2.5. Scanning electron microscope

Scanning electron microscopy (SEM) was carried out by SEM-EDS to characterize the microstructure and particle morphology of the fly ash. The analysis was done under pressure of 90 Pa and a resolution of <10 nm at 20 kV. This analysis was performed in the laboratory of innovation of Fez city.

2.2.6. X-ray diffraction analysis

X-ray diffraction (XRD) analysis was performed to determine the composition of our adsorbent material using rotating anode Cu Kα (1.54060 Å). This analysis was also carried out in the innovation laboratory of Fez city.

2.2.7. Chemical elements

After mineralization by acid, mineral elements of fly ash were identified by atomic absorption spectroscopy (ICP) in the innovation laboratory of Fez city.

2.3. Adsorption test

2.3.1. Influence of adsorption parameters

The adsorption capacity of fly ash was assessed for removing COD, sulfide ions and chromium VI from the tannery effluent. All adsorption experiments were evaluated in batch mode and conducted in 150 mL of tannery effluent. The effect of several parameters was studied and optimized, which were adsorbent dosage (0.05–2 g/L), solution pH (2–12), agitation speed (50–200 rpm with 50 intervals), temperature (20–60 °C with ten °C intervals) and contact time (0–60 min).

2.3.2. Adsorption kinetics

Kinetic experiments were conducted by mixing two g/L fly ash with 150 mL of tannery effluent. The suspensions were shaken using optimal parameters for 60 min. Samples were progressively taken and assessed. The following three equations (pseudo-first order, Equation (1); pseudo-second-order, Equation (2); Elovich, Equation (3)) were analyzed to fit the experimental kinetic data. The best fit of the kinetic model was estimated according to regression coefficient values (R^2) obtained from a linear plot of each equation model.

$$\ln(q_e - q) = \ln(q_e) - \frac{k_1}{2.303} * t \quad (1)$$

$$\frac{t}{q} = \frac{1}{k_2 * q_e^2} + \frac{1}{q_e} * t \quad (2)$$

$$q = \frac{1}{\beta}\ln(\alpha.\beta) + \frac{1}{\beta} * \ln(t) \quad (3)$$

where, qe and q are the adsorbed amount (mg/g) at an equilibrium concentration (Ce, mg/g) and a designated time (t, min) within the solutions, respectively. k_1 and k_2 are the rate constants for the pseudo-first-order model (1/min) and pseudo-second-order model (g/mg/min); respectively.α (mg/g/min) is initial sorption speed. β (g/mg) is desorption constant.

2.3.3. Adsorption isotherms

Adsorption isotherm studies were performed by subjecting different adsorbent masses (0.05–2 g/L) to 150 mL of tannery effluent at 25 °C and using optimal pH and agitation speed parameters. Langmuir and Freundlich's models were also investigated for adsorption isotherm modelling of the experimental data, and the correlation coefficients R^2 were employed to determine the best-fitting isotherm. Equations (4) and (5) describe Langmuir and Freundlich models, respectively.

$$\frac{C_e}{q_e} = \frac{1}{q_m} * C_e + \frac{1}{K_L * q_m} \tag{4}$$

$$\ln(q_e) = \ln(K_F) + \frac{1}{n} * \ln(C_e) \tag{5}$$

The model of Langmuir is valid for monolayer surface adsorption, where qm (mg/g) indicates the maximal adsorption capacity and K_L (L/mg) reflects the adsorption energy. Otherwise, the empirical Freundlich isotherm is applied for heterogeneous adsorption, where the interaction between adsorbed molecules could be implemented. The parameter (n) indicates the heterogeneity factor, so the adsorption may be linear (n = 1), chemically (n < 1), or physically (n > 1). Furthermore, 1/n < 1 indicates a Langmuir model while 1/n > 1 is for cooperative adsorption [24]. K_F is the adsorption capacity ($mg^{1-1/n}\ L^{1/n}/g$), qe (mg/g) is the amount of dye adsorbed per unit weight of adsorbent, and Ce (mg/L) is the equilibrium concentration of solute.

2.3.4. Thermodynamic study

The thermodynamic study was also undertaken to identify the enthalpy (ΔH°), entropy (ΔS°) and free energy (ΔG°). This study was carried out at different temperatures keeping all other parameters constant. The thermodynamic functions were determined from the following Equations (6)-(9).

$$\text{Van}'\text{tHofff}\Delta G^\circ = -RT\ln(K_D) \tag{6}$$

$$K_D = \frac{C_e}{q_e} \tag{7}$$

$$\Delta G^\circ = \Delta H^\circ - T\Delta S^\circ \tag{8}$$

$$\ln(k_D) = \frac{\Delta S^\circ}{R} - \frac{\Delta H}{RT} \tag{9}$$

K_D is the equilibrium constant, R is the gas constant, and T is the absolute temperature. The plot $\ln(k_D)$ versus 1/T was used to calculate ΔH° and ΔS° to understand the nature of adsorption. The thermodynamic parameters can be calculated from the equilibrium constant K_D (Ce/qe).

2.4. Analysis method

As mentioned, the adsorption treatment study was assessed by following the COD, sulfide ions and Cr(VI) concentration. For that, several aliquots of the effluent were filtered using a filter paper; then, the final concentrations of the studied parameters were measured according to the standard method described by Rodier [18].

Then, their adsorbed amount (q) and abatement rate were calculated using the following Equations (10) and (11):

$$q_e = \frac{(C_0 - C_e)}{W} * V \tag{10}$$

$$\text{Removal}\ (\%) = \frac{(C_0 - C_e)}{C_0} * 100 \tag{11}$$

where q_e is the adsorption capacity (mg/g), C_0 is the initial parameter concentration (mg/L), Ce is the equilibrium parameter concentration within the effluent (mg/L), V is the volume of the tannery effluent (L), m is the weight of the adsorbent in g.

All experiments were done in triplicate to ensure the accuracy of our results; the relative standard deviation was estimated to be within ±1.5% of the presented average values.

3. Results and discussions

3.1. Fly ash characterisation

3.1.1. Iodine number

The iodine number indicates material porosity, so the highest iodine value suggests that the material is very porous. As for fly ash, the iodine number was 837.54 mg/g. This value is attractive and reflects the high porosity of our material. This iodine value is higher than many other materials, including commercial activated carbon (Table 2). Thus, fly ash may be promising and may replace those

expensive materials.

3.1.2. pH at the point of zero charge

Fig. 2 shows the plot of ΔpH versus pHi, and demonstrates the pHpzc of fly ash wherein the surface will be neutral. According to this Figure, the pHpzc of fly ash is 9.78. So, the surface becomes positively charged when effluent pH < pHpzc, and negatively charged when effluent pH > pHpzc.

3.1.3. Specific surface area and pore structure

Adsorptive capacity is an essential property of the adsorbent and is related to the specific area.Table 3 presents the obtained results of specific surface area (S_{BET}) and pore structure of fly ash. As shown, fly ash has a very high specific surface, a high volume of mesoporous compared to microspores and an average pore diameter of 35 Å. Moreover, the pore volume value confirms the result of the iodine number. Therefore, fly ash generally has a mesoporous structure but with a good percentage of microspores. According to Krou [29], mesoporous material can be excellent adsorbents.

On the other hand, Table 4, shows the specific surface of some commercialized industrial adsorbents and their porosity. Consequently, fly ash has a high S_{BET} compared to these adsorbents. This confirms that fly ash can replace commercial activated carbon due to its interesting physical properties.

3.1.4. Fly ash morphology by SEM

The SEM result is reported in Fig. 3(a and b). Fly ash has spherical granules with different particle sizes ranging between 32 nm and 100 μm according to the SEM. This small particle size of fly ash could explain the high percentage of pores obtained by BET analysis and, subsequently, the high specific surface. As well, the volume of mesopores appears more dominant compared to micropores volume. Otherwise, the particle size of our fly ash is smaller comparing to those found by Basava Rao et al. who worked on the adsorption onto two different samples of fly ash [17].

3.1.5. Chemical composition of fly ash

The chemical composition results are presented in Table 5. Silica oxide is the most dominant component, followed by aluminum oxide. Moreover, the sum of SiO_2 + Al_2O_3 + Fe_2O_3 is about 94.21%, which is comparable to those found by El Fadel [16]. Consequently, fly ash is among silico-aluminous materials. According to various studies, silica and aluminum are among the most efficient adsorbents. On the other hand, the silicon-aluminous percentage of our fly ash is higher than that found in another study on fly ash using two different samples, in which both of them had a silicon-aluminous percentage less than 90% [17].

3.1.6. X-ray diffraction analysis

The XRD diffractogram of fly ash is reported in Fig. 4. Diffractogram reveals the presence of two peaks, which are mullite ($Al_6Si_2O_{13}$) and quartz (SiO_2). These results are in accordance with the ICP results mentioned above, and they are similar to those found by El Fadel [16]. In addition, these results showed that these fly ashes resemble others in Spain and other countries [31,32].

Indeed, the composition of the fly ash depends on the original coal. Therefore, these results can be explained by the mineralogy of the combusted coal, which is composed of crystallized silica in the form of quartz and phyllite minerals of the clay group (shales). These minerals change their structure during the combustion, giving rise to a crystallized part in the form of mullite and quartz. The latter does not change its structure and remains in its initial state [16].

3.2. Optimization of adsorption process

3.2.1. Effect of contact time

Fig. 5(a–c) demonstrates the effect of contact time on the adsorption of COD, chromium VI and sulfide ions from the composite tannery effluent. As shown, all parameters' adsorption speeded during the first 10 min. The removal rates were 73.95%, 80% and 85% for COD, Cr (VI) and sulfides, respectively. Then, an increase followed by a stabilization of these abatement rates was revealed for these three parameters. The stabilization is proven from 30 min, where the abatement rates were 86%, 92% and 95% for COD, Cr (VI) and sulfides, respectively. Therefore, 30 min can be considered the optimal and equilibrium time. The availability of active adsorption sites could explain these results pending the initial stage, so the pollutants are easily accessible and adsorbed. After a lapse of time, these sites become saturated, and the diffusion or the adsorption becomes slow [33].

Some researchers studied the adsorption of chromium Cr(VI) onto eggshell, and showed that the equilibrium contact time was 110

Table 2
Iodine number of some materials.

Material	Iodine number (mg/g)	References
Fly ash	837.54	This study
Coconut activated with phosphoric acid (10%)	503	[25]
coffee grounds activated with $ZnCl_2$ and H_3PO_4	460	[26]
Commercial activated carbon	500	[27]
Olive seeds activated with phosphoric acid (10%)	571	[28]

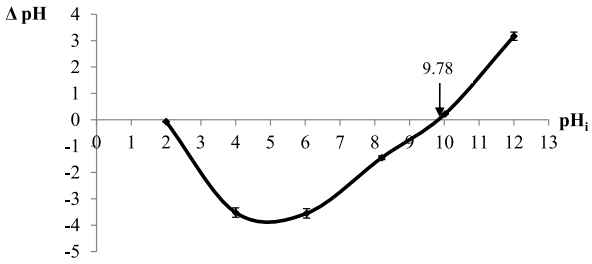

Fig. 2. pH at the point of zero charges of fly ash.

Table 3
S_{BET} and pore structure results of fly ash.

	S_{BET} (m^2/g)	V_{mic} (cm^3/g)	V_{meso} (cm^3/g)	V_T P (cm^3/g)	D_M P (Å)
Fly ash	3127.2	1.02	2.15	3.27	35

V_{mic}: micropores volume.
V_{meso}: mesopores volume.
V_T P: Total pore volume.
D_M P: Average pore diameter.

Table 4
Characteristics of some industrial adsorbents [30].

	Specific area (m^2/g)	Pore diameter (nm)	Interne Porosity (Vmicro pores/Vt)
Activated carbon	400–2000	1–4	0.4–0.8
Zeolites	500–800	0.3–0.8	0.3–0.4
Silica gels	600–800	2–5	0.4–0.5
Activated aluminas	200–400	1–6	0.3–0.6

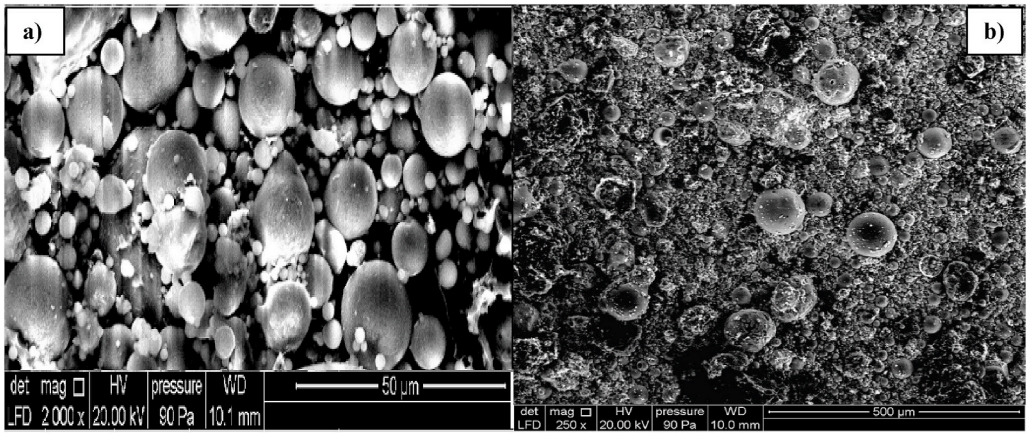

Fig. 3. Fly ash morphology by SEM (a: Zoom 2000×; b: Zoom 250×).

Table 5
Chemical composition of fly ash by ICP.

Chemical elements	SiO_2	Al_2O_3	Fe_2O_3	CaO	MgO	SO_3	K_2O
Percentage (%)	66.12	26.05	2.04	0.51	0.31	0.50	0.48

min using 12 g/L as adsorbent dose [34]. The removal of Cr (VI) by adsorption onto tea waste was investigated, and the equilibrium contact time was between 50 and 150 min [13,14]. Therefore, the equilibrium contact time of our fly ash is very lower than those low-cost adsorbents.

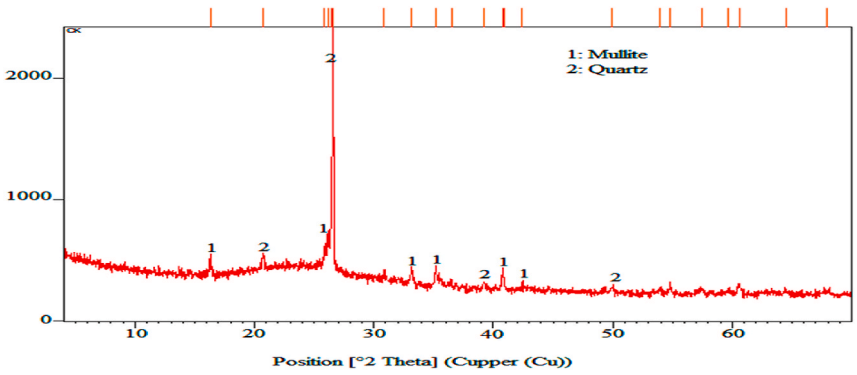

Fig. 4. XRD diffract gram of fly ash.

3.2.2. *Effect of adsorbent mass*

Fig. 6(a–c) indicates the impact of fly ash mass. As shown, the removal of the three parameters increases with the increase of the adsorbent dose used. From 0.25 g to 2 g, the abatement rate increased from 48% to 96% for COD, from 43% to 97.5% for hexavalent chromium and from 45% to 97.2% for sulfide ions. This result is in accordance with several studies [35].This could be explained by the increase of adsorption sites when the adsorbent mass increases too [36]. It also increases the specific surface area and achieves the best purifying capacity [37].

3.2.3. *Effect of pH*

Fig. 7(a–c) represents the influence of pH on removing COD, Cr(VI) and sulfide ions. pH plays a crucial role in the adsorption phenomenon because it can change the charge of the material surface, the degree of dissociation of the functional groups of the active sites and the degree of ionization of the adsorbent [38].

For COD (Fig. 7(a)), its removal rate increases from 63% to 92.2% when the pH varies from two to nine. At this stage, the pH is lower than pHpzc (9.78), so the fly ash surface is positively charged and captures all negatively charged molecules. Then, the surface is progressively deprotonated by increasing the pH from 2 to 9; this leads to the release of adsorption sites and allows large molecules to adsorb as well [39]. On the other hand, a decrease in abatement rates was observed when pH exceeded 9. This could be related to the surface charge, which will be negatively charged as the pH becomes higher than 9.78 (pHpzc). Therefore, electrostatic repulsion dominates between the adsorbate and the adsorbent surface.

Regarding chromium VI (Fig. 7(b)), Cr(VI) removal reached 90% at pH 2, and then it decreased progressively as the pH increased.

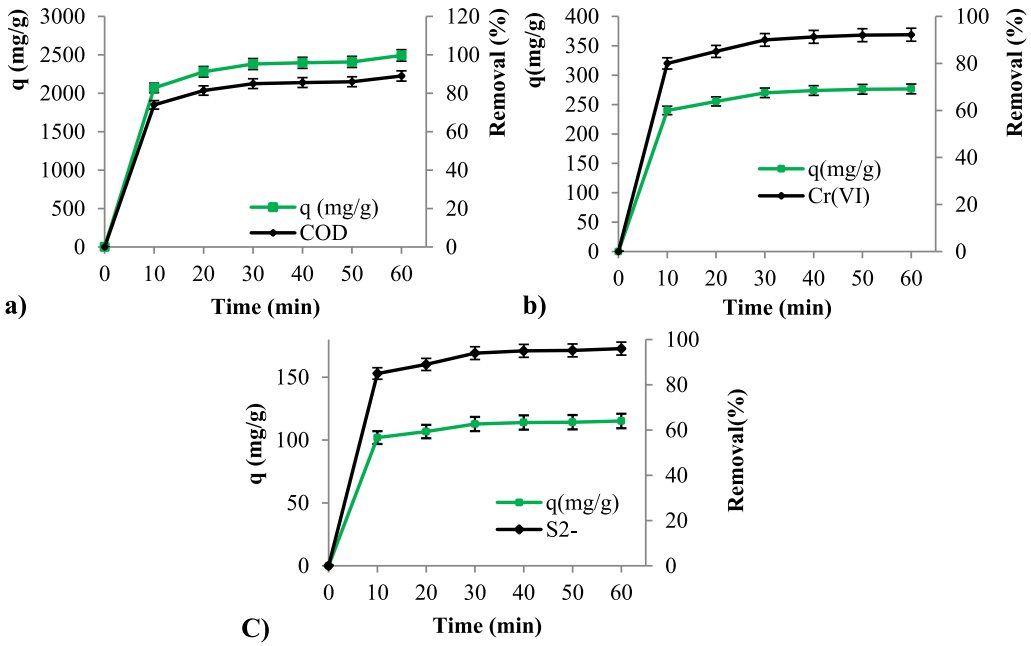

Fig. 5. Effect of contact time on q (mg/g) and removal of: a) COD; b) Cr(VI); c) S^{-2}; (Adsorbent dose = 0.5 g/L; Temperature = 30 °C; pH = 8; Volume = 0.2 L; Stirring speed = 100 tr/min).

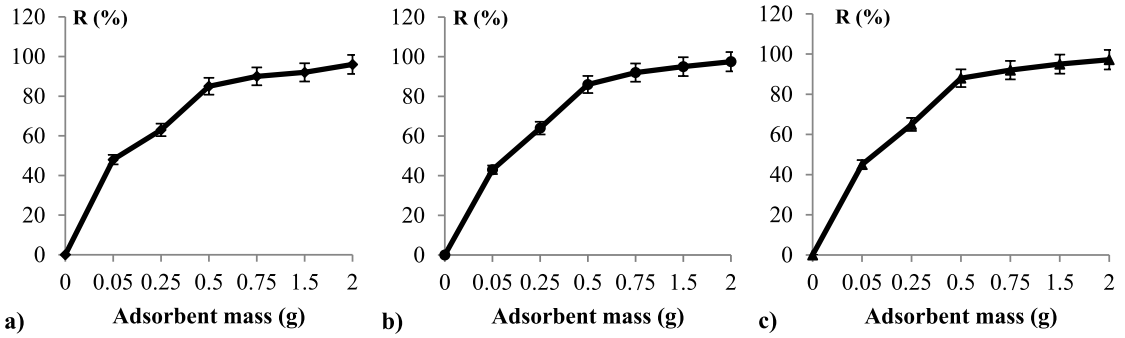

Fig. 6. Optimization of the adsorbent mass: a) COD; b) Cr(VI); c) S^{-2}; (R = Removal; Operating conditions: Contact time = 30 min; Temperature = 30 °C; pH = 8; Volume = 0.2 L; Stirring speed = 100 rpm).

Indeed, pH is the most important parameter when assessing the efficiency of an adsorbent for metal ion removal because it influences material surface properties and ionic forms of metal. Moreover, in the pH range of 2.0–6.0, chromium ions co-exist in different forms, such as $Cr_2O_7^{2}$, $Cr_3O_{10}^{2}$, $Cr_4O_{13}^{2}$ and $HCrO_4$, which predominates. Thus, the adsorbent surface was highly protonated at acidic pH, which significantly caused a strong electrostatic attraction between positive charges of the adsorbent surface and chromate ions. Otherwise, the predominant species are CrO_4^{2} and $Cr_2O_7^{2-}$ at the pH range of 6–9. So, lesser adsorption was observed at this range, which may be due to the dual competition of both anions (CrO_4^{2} and OH^-) to be adsorbed because OH^- predominates as increasing the pH. This could explain the sharp decline of chromium removal at pH values greater than 6. These results are in accordance with various studies [40, 41].

The impact of pH on sulfide removal is depicted in Fig. 7(c). Like chromium hexavalent, a decline in sulfide ions uptake was observed, achieving 94% as the highest removal at pH 2. As chromium, sulfide takes different forms depending on the pH of the effluent, in which the majority of these forms have a negative charge. Therefore, sulfide adsorption is related to the adsorbent surface charge; hence, the abatement rate of sulfides is high when the surface is strongly protonated at lower pH.

Considering the above, pH 8 can be the optimal pH for COD removal, whereas pH 2 can be the best for the high uptake of Cr (VI) and sulfide ions.

3.2.4. *Effect of temperature*

Experiments are done at different temperatures (20, 30, 40, and 50 °C) applying the following conditions: adsorbent dose (1 g/L), agitation time (60 min), agitation speed (100 tr/min); Volume = 0.2 L; pH = 8. The influence of temperature is shown in Fig. 8(a–c), wherein a slight increase in the abatement rates of three parameters is revealed as the temperature increases too. The equilibrium is achieved at 30 °C, where the highest removals were depicted, and they were 86%, 93% and 94%, respectively, for COD, chromium VI and sulfide ions. These results could be explained by the increase of the sorbate's diffusion rate within the pores as the temperature increased. A similar result has been observed in the case of activated carbon too. Furthermore, these fly ash results conform to others in India [17].

3.2.5. *Effect of agitation speed*

The effect of stirring speed was studied after fixing the contact, temperature, adsorbent mass, volume, and pH = 8 (Fig. 9(a–c)). The removal of the three studied parameters was demonstrated when the stirring speed varies from 50 to 100 rpm. When the stirring speed

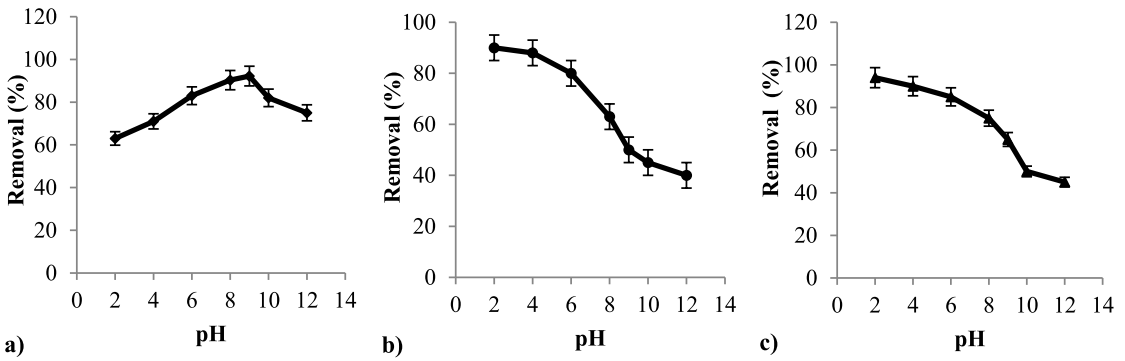

Fig. 7. Optimization of pH: a) COD; b) Cr(VI); c) S^{-2}; (Operating conditions: Contact time = 30 min; Temperature = 30 °C; Adsorbent mass = 1 g/L; Volume = 0.2 L; Stirring speed = 100 rpm).

exceeds 100 rpm, these removal rates become constant or slightly decreased. Thus, the agitation speed of 100 tr/min was considered optimal, wherein the abatement rates achieved 90%, 93% and 94% for COD, Cr (VI) and sulfide ions, respectively.

3.3. Adsorption kinetics

Several kinetic models may be investigated to control the mechanism of the adsorption process. In this study, three common models predicted the adsorption kinetics: pseudo-first-order, pseudo-second-order and Elovich models. The results are depicted in Table 6.

As shown, the regression coefficient of the pseudo-second-order model is very high and close to 1 compared to those of the first-order and Elovich, and qe calculated by the pseudo-second-order model is near to qe calculated through experiments. This pseudo-second-order model indicates that chemical interactions between fly ash and molecules may be present during the adsorption phenomenon. The regression coefficients of the Elovich model are also more significant; this may indicate that the surface is heterogeneous. Consequently, the adsorption of these pollutants by fly ash may be chemical and physical simultaneously. In fact, the physical adsorption could be performed after the saturation of the active adsorption sites, in which the molecules will diffuse into fly ash pores. This phenomenon is slower than chemical interactions [42]. These results are similar to those found by other researchers [39,43].

Fig. 10(a and b) shows the tannery effluent before and after adsorption onto fly ash. Hence, this figure could highlight the strong adsorption capacity of this waste, in which the removal of COD, and sulfide were 93.3%, and 97.2% respectively. Those abatement rates are higher than other founded by other researchers [13,44].

Table 7, depicts the chromium VI adsorption potential of some low-cost adsorbents including fly ash. As shown, fly ash is more powerful and has a high Cr (VI) adsorption capacity reached to 223.7 mg/g.

3.4. Adsorption isotherms

3.4.1. Adsorption type

To determine the adsorption type adopted by fly ash, the plot of the concentration (Ce (mg/L)) versus adsorbed amount (qe (mg/g)) were traced for COD, Cr (VI) and S^{2-}, and then the results are shown in Fig. 11(a–b). As demonstrated, an upward concavity was observed for all three parameters. Taking this into consideration and the Giles classification [47], the fly ash adsorption follows S-type. This type indicates the presence of multilayer adsorption. So, adsorbed molecules promote the adsorption of other molecules when the solute concentration is higher (Cooperative Adsorption). The attraction of these molecules could explain this by Van Deer Wals forces, and then they regrouped as flocs [48]. Smectites (montmorillonites) or other clays [49] often adopt this adsorption type. According to Bouzid [50], the adsorption of organic substances by organic-poor materials is generally characterised by this isotherm S. This is thus in accordance with our results.

3.4.2. Isotherm models

According to Baccar [51], the isotherm study shows how the adsorbed molecules are distributed in the solid phase in equilibrium. For this reason, two main isotherm models have been studied: the Langmuir and Freundlich models. Indeed, this study is done at pH 8, temperature 30 °C, under a stirring speed of 100 rpm. The constant parameters qm, K_L, n, K_F, and the regression coefficients R^2 were calculated and presented in Table 8.

According to the Langmuir model, qm of COD, Cr (VI) and S^{2-} is 2100 mg/g, 200.02 mg/g and 99.89 mg/g, respectively. These values are lower than experimental values, and this indicates that the adsorption is not monolayer only. The obtained K_L values are less than 1; this suggests that the physical adsorption is favorable [52]. Otherwise, the Freundlich model gives the highest R^2 values compared to the Langmuir model. Consequently, it is evident that the adsorption mechanisms followed this model.

According to Freundlich's theory, there is a possibility of forming one or more layers on the surface. As well, it indicates that the sites are heterogeneous with different binding energies. In addition, the n values are less than 1, revealing that the adsorption may be chemical [53]. Furthermore, the 1/n values are also greater than 1, indicating that the type of adsorption is S-type, which is ideally in conformity with our previous results. This result is different from that obtained in previous studies on adsorption onto fly ash, wherein Langmuir model gave a better fit for the experimental adsorption equilibrium data [17]. This could be explained by the difference of fly ash characteristics used in our study and theirs.

3.5. Thermodynamic isotherm

Obviously, thermodynamic parameters can influence the adsorption process, so the Van't Hoff model studied the thermodynamic isotherm.

The thermodynamic parameters (ΔG^0, ΔH^0, and ΔS^0) were calculated, and the results are demonstrated in Table 9.

As shown in the table above, ΔS^0 values are positive and oscillate around 0.03 kj/mol/K; subsequently, it indicates an increase of randomness at the solid-solute interface during the adsorption. It thus assumes this phenomenon's high stability without changes in the structure of the solid/liquid interface [54]. This can be explained as follows: the adsorbed molecules displace adsorbed molecules to gain more energy than was lost by adsorbate, allowing randomness in the system [39]. Positive values of ΔH^0, which varies between 0.5 and 4.12 kj/mol, confirm that the adsorption process is endothermic [55]. Finally, negative values of ΔG^0 indicate the feasibility and spontaneity of the adsorption onto fly ash. Moreover, the decrease in ΔG^0 shows the feasibility of adsorption at high temperatures. Li using activated carbon [56] demonstrated similar results.

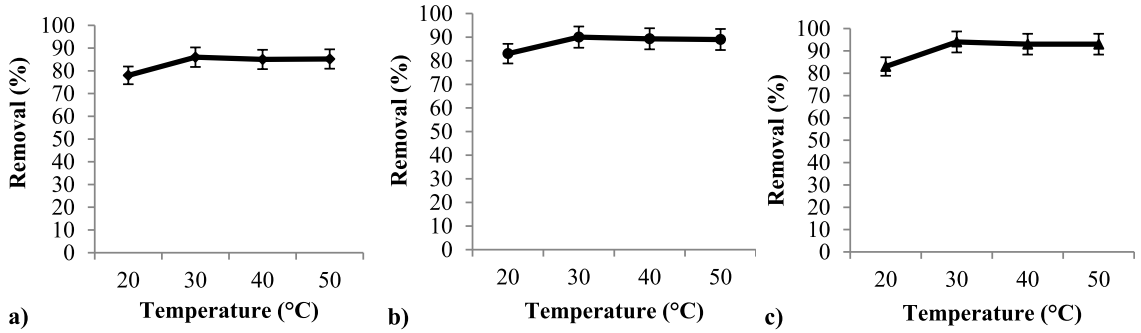

Fig. 8. Temperature optimization: a) COD; b) Cr (VI); c) S^{-2}; (Operating conditions: Contact time = 30 min; Stirring speed = 100 rpm; Adsorbent mass = 1 g/L; Volume = 0.2 L; pH = 8).

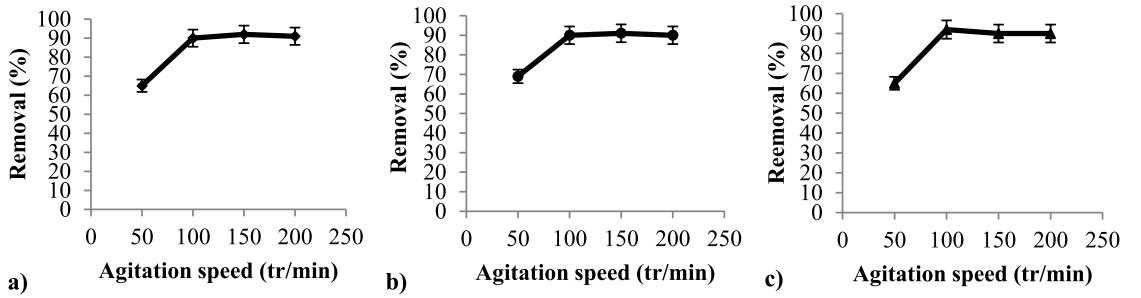

Fig. 9. Optimization of the stirring speed: a) COD; b) Cr (VI); c) S^{-2}; (Operating conditions: Contact time = 30 min; Temperature = 30 °C; Adsorbent mass = 1 g/L; Volume = 0.2 L; pH = 8).

Table 6
Constant parameters and correlation coefficients (R^2) calculated for the pseudo-first order, pseudo-second order and Elovich kinetic models.

qe (exp) (mg/g)		COD	Cr(VI)	S^{2-}
		2496	223.7	106.8
Pseudo-first order	K_1 (min^{-1})	0.242	0.076	0.06
	qe (cal) (mg/g)	12.4	5.4	2.65
	R^2	0.911	0.87	0.79
Pseudo-second order	K_2 (g/mg min)	0.000032	0.0022	0.005
	qe (cal) (mg/g)	2500	250	111.11
	R^2	0.999	0.999	0.999
Elovich	α(g/g min)	16.27	415.9	397.96
	β (g/mg)	0.0016	0.027	0.06
	R^2	0.978	0.932	0.929

4. Conclusion

The present work focused on the valorisation of fly ash, the waste of power stations, into a raw adsorbent for treating tannery effluent in Morocco. The physicochemical characterisation revealed perfect proprieties manifested by high porosity, great S_{BET}, a considerable percentage of silica and aluminum, and an alkaline pHpzc. In batch mode studies, fly ash was shown to have a strong purification capacity. The maximum sorption capacity achieved 2496, 223.7, and 106.8 mg/g for COD, Cr(VI), and sulfide ions in 30 min is an equilibrium time. Among the kinetics model, the adsorption onto fly ash fits perfectly with the pseudo-second-order model. Equilibrium data significantly correlated with the Freundlich sorption model, showing cooperative adsorption and heterogeneous distribution of active sites on the fly ash surface.

Furthermore, thermodynamic parameters show an endothermic and spontaneous adsorption process, which is more favorable with increasing temperature. In conclusion, fly ash has established an excellent adsorption potential, even at lower doses, due to its strong physicochemical characteristics being more excellent than commercial activated carbon and other expensive industrial adsorbents. This valorisation will also be a promising, attractive and eco-friendly strategy for treating tannery effluent or any other industrial wastewaters, as it can be the best solution for managing this solid waste that harms our environment.

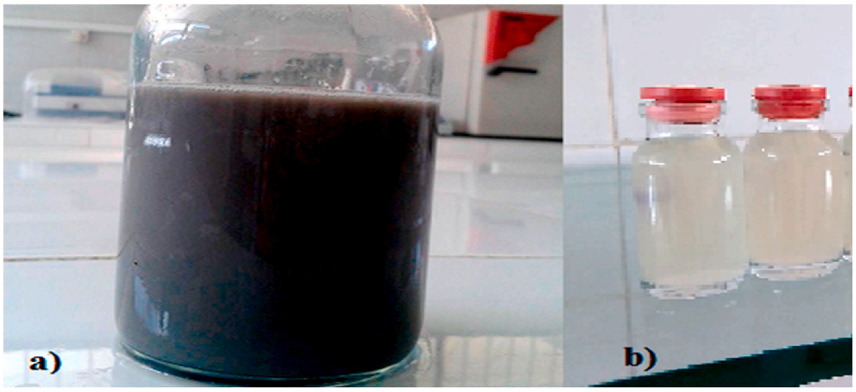

Fig. 10. Tannery effluent before (a) and after (b) adsorption onto fly ash using batch experiment.

Table 7
Comparison of Cr(VI) adsorption capacity of fly ash with other low-cost adsorbents.

Adsorbent	qe (mg/g)	References
PEI functionalized Eggshell	160	[45]
Jatropha Wood	140.8	[45]
Soy hull biomass	7.29	[46]
Sulphuric acid modified pine sawdust	20.3	[45]
Zizania caduciflora	2.70	[45]
Cement dust	33	[15]
Tea waste	10.64	[14]
Fly ash	223.7	This study

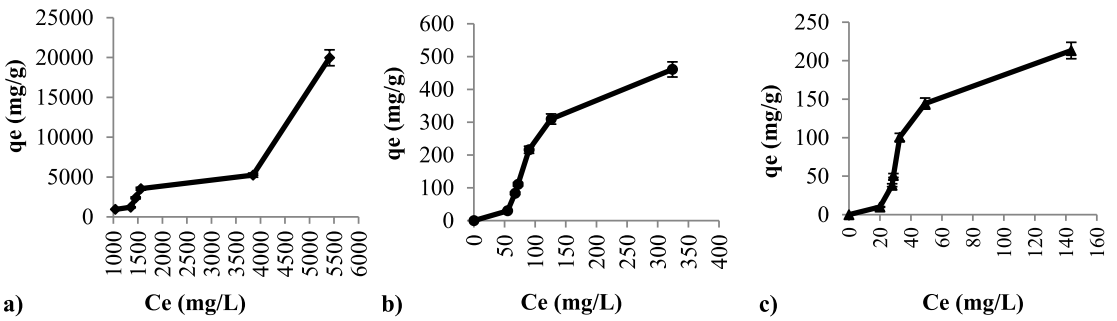

Fig. 11. Fly ash adsorption type according to Gile classification a) COD; b)Cr (VI); c) S^{-2}.

Table 8
Isotherm constants for adsorption onto fly ash.

qe (exp) (mg/g)		COD	Cr(VI)	S^{2-}
		2496	223.7	106.8
Langmuir model	K_L (L/mg))	0.00034	0.0135	0.0166
	qm (cal) (mg/g)	2100	200.02	99.89
	R^2	0.75	0.873	0.774
Freundlich model	K_F (L/mg)	0.18	0.87	1.15
	n	0.637	0.84	0.9
	R^2	0.978	0.986	0.98

Author contributions

Supervision, Prs Merzouki Mohammed and Mohamed Benlmelih. Software, Laidi Omar. Methodology, Fatima Atia and Anass Omor.Writing, methodology and formal analysis, Elkarrach Karima.

Table 9
Thermodynamic parameters of COD, Cr (VI) and S^{2-} adsorption onto fly ash.

	Temperature (K)	ΔH° KJ/mol	ΔS° Kj/mol/K	ΔG° Kj/mol
COD	293	0.55	0.033	−9.12
	303			−9.45
	313			−9.78
	323			−10.11
Cr(VI)	293	4.12	0.037	−6.87
	303			−7.24
	313			−7.62
	323			−7.99
S^{2-}	293	3.58	0.031	−5.51
	303			−5.81
	313			−6.12
	323			−6.43

Availability data

The authors confirm that the data supporting the findings of this study are available within the article.

Declaration of competing interest

The authors declare no conflict of interest.

Acknowledgements

The authors would like to acknowledge the staff of Innovation Laboratory in Fez city for the crucial facilities and support provided to carry out the characterisation of fly ash. We would also like professors and PhD students of the Department of Industrial Engineering of Padova University in Italy for their help and cooperation.

References

[1] A. Omor, K. Elkarrach, R. Ouafi, O. Laidi, M. Merzouki, K. El Rhazi, Z. Rais, Prevalence of ORL and dermatitis diseases among tanners in Fez-Morocco: association with risk factors and working sections, J. Toxicol. Anal. Clin. 34 (2022) 262–267, https://doi.org/10.1016/j.toxac.2022.07.001.
[2] K. Elkarrach, M. Merzouki, O. Laidi, S. Biyada, A. Omor, M. Benlemlih, Sequencing batch reactor: inexpensive and efficient treatment for tannery effluents of Fez City in Morocco, Desalination Water Treat. J 203 (2020) 1–7, https://doi.org/10.5004/Dwt.2020.26151.
[3] K. Elkarrach, M. Merzouki, S. Biyada, M. Benlemlih, Bioaugmentation process for the treatment of tannery effluents in Fez, Morocco: an eco-friendly treatment using novel chromate bacteria, Water Process. Eng. J. 38 (2020) 101–589, https://doi.org/10.1016/J.Jwpe.2020.101598.
[4] A. Omor, Z. Rais, K. El Rhazi, M. Merzouki, K. Elkarrach, N. Elallaoui, M. Taleb, Optimization of the method wastewater treatment of unit bovine hides's unhairing liming, J.M.E.S. 8 (4) (2017) 1235–1246.
[5] G. Boczkaj, A. Fernandes, Wastewater treatment by means of advanced oxidation processes at basic pH conditions: a review, Chem. Eng. J. 15 (2017) 608–633, https://doi.org/10.1016/j.cej.2017.03.084.
[6] P. Asaithambi, R. Govindarajan, M.B. Yesuf, P. Selvakumar, E. Alemayehu, Investigation of direct and alternating current-electrocoagulation process for the treatment of distillery industrial effluent: studies on operating parameters, J. Environ. Chem. Eng. (2020), https://doi.org/10.1016/j.jece.2020.104811.
[7] T.G. Kebede, A.A. Mengistie, S. Dube, T.T.I. Nkambule, M.M. Nindi, Study on adsorption of some common metal ions present in industrial effluent by *Moringa stenopetala* seed powder, J. Environ. Chem. Eng. 6 (1) (2017) 1378–1389, https://doi.org/10.1016/j.jece.2018.01.012.
[8] M.C. Pire-Sierra, D.D. Cegarra-Badell, S.J. Carrasquero-Ferrer, N.E. Angulo-Cubillan, A.R. Díaz-Montiel, Nitrogen and COD removal from tannery wastewater using biological and physicochemical treatments, Rev. Fac. Ing., Univ. Antioquia 80 (2016) 63–73, https://doi.org/10.17533/udea.redin.n80a08.
[9] S. Mustapha, M.M. Ndamitso, A.S. Abdulkareem, J.O. Tijani, A.K. Mohammed, D.T. Shuaib, Potential of using kaolin as a natural adsorbent for the removal of pollutants from tannery wastewater, Heliyon 5 (11) (2019), e02923, https://doi.org/10.1016/j.heliyon.2019.e02923.
[10] Y. Sandeep, S. Varsha, B. Sushmita, W. Chih-Huang, C.S. Yogesh, Adsorption characteristics of modified sand for the removal of hexavalent chromium ions from aqueous solutions: kinetic, thermodynamic and equilibrium studies, CATENA 100 (2013) 120–127, https://doi.org/10.1016/j.catena.2012.08.002.
[11] G. ElMouhri, M. Merzouki, Y. Miyah, K. Elkarrach, F. Mejbar, R. Elmountassir, A. Lahrichi, Valorization of two biological materials in the treatment of tannery effluents by filtration, Mor. J. Chem. 7 (1) (2019) 183–193, https://doi.org/10.48317/IMIST.PRSM/morjchem-v7i1.14064.
[12] R.E.H. El-Sayed, M. Rostom, F.E. Farghaly, M.A. Abdel Khalek, Bio-sorption for tannery effluent treatment using eggshell wastes; kinetics, isotherm and thermodynamic study. Egypt, J. Petrol. 29 (2020) 273–278, https://doi.org/10.1016/j.ejpe.2020.10.002.
[13] M. Swathi, A.S. Sathya, S. Aravind, P.K.A. Sudhakar, R. Gobinath, D. Devi Saranya, Adsorption studies on tannery wastewater using rice husk, SJET 2 (2B) (2014) 253–257.
[14] M. Nur-Alam, M.A.S. Mia, M.M. Rahman, COD removal of tannery wastewater using spent tea leaves, IRJET 4 (11) (2017) 1940.
[15] O.A. Fadali, Y.H. Magdy, A.A.M. Daifullah, E.E. Elbrahiem, M.M. Nasser, Removal of chromium from tannery effluents by adsorption, J. Environ. Sci. Health, Part A-Toxic/Hazar. Subst. Environ. Eng. 2 (2004) 465–472, https://doi.org/10.1081/ESE-120027537.
[16] H. El Fadel, Traitement Physico-Chimique Et Biologique Des Lixiviats De La Décharge Publique Contrôlée De La Ville De Fès : Application Des Procédés De Filtration, Coagulationfloculation Et Du SBR (Leachates Physical-Chemical and Biological Treatment of the Controlled Landfill of Fez City: Application of Filtration, Coagulation-Flocculation and SBR Processes), Thesis Faculty of Sciences Dhar El Mahraz, Sidi Mohamed Ben Abdellah University Fez- Morocco, 2013.
[17] V.V. Basava Rao, S.M. Mohan Rao, Adsorption studies on treatment of textile dyeing industrial effluent by flyash, Chem. Eng. J. 116 (2006) 77–84, https://doi.org/10.1016/j.cej.2005.09.029.
[18] J. Rodier, Analysis of Water – Fresh Water, Wastewater, Seawater, ninth ed., 2009. Dunod, Paris.
[19] K. Elkarrach, M. Merzouki, O. Laidi, A. Omor, S. Biyada, M. Benlemlih, Combination of chemical and biological processes for the treatment of tannery effluent of Fez city in Morocco, Desalination Water Treat. J. 220 (2021) 109–115, https://doi.org/10.5004/dwt.2021.26989.
[20] State Secretariat for Water and Environment, Moroccan Laws Relating to the Environment, in: Official bulletin, n° 6199 du 22 hija 1434, Department of the Environment, Morocco, 2013.

[21] ASTM D4607-86, Standard Test Method for Determination of Iodine Number of Activated Carbon, Available online at: http://www.astm.org/Standards/D4607.htmAccessed on 14-05-11, 2006.

[22] F.R. Furlan, L.G. Silva, A.F. Morgado, A.A.U. Souza, S.G. Souza, Removal of reactive dyes from aqueous solutions using combined coagulation/flocculation and adsorption on activated carbon, Resour. Conserv. Recycl. J. 54 (5) (2010) 283–290, https://doi.org/10.1016/j.resconrec.2009.09.001.

[23] M.A. Slasli, Modélisation de l'adsorption par les charbons microporeux: Approches théorique et expérimentale (Modeling adsorption by microporous carbons: theoretical and experimental approaches), Neuchâtel University, Switzerland, 2002.

[24] A.M. Vargas, A.L. Cazetta, M.H. Kunita, T.L. Silva, V.C. Almeida, Adsorption of methylene blue on activated carbon produced from flamboyant pods (Delonix regia): study of adsorption isotherms and kinetic models, Chem. Eng. J. 168 (2011) 722–730, https://doi.org/10.1016/j.cej.2011.01.067.

[25] M. Gueye, J. Blin, C. Brunschwing, Study of the Synthesis of Activated Carbons from Local Biomasses by Chemical Activation with H_3PO_4, in: Scientific Days of Ouagadougou Campus, 2011, pp. 4–8.

[26] A. Namane, A. Mekarzia, K. Benrachedi, N. Belhaneche-Bensemra, A. Hellal, Determination of the adsorption capacity of activated carbon made from coffee grounds by chemical activation with $ZnCl_2$ and H_3PO_4, J. Hazard Mater. 119 (2005) 189–194, https://doi.org/10.1016/j.jhazmat.2004.12.006.

[27] A. Maleki, M.B.K. Erfan, A.S. Mohammadi, R. Ebrahimi, Application of commercial powdered activated carbon for adsorption of carbolic acid in aqueous solution, Pakistan J. Biol. Sci. 10 (14) (2007) 2348–2352, https://doi.org/10.3923/pjbs.2007.2348.2352.

[28] F. Benamraoui, Elimination Des Colorants Cationiques Par Des Charbons Actifs Synthétisés A Partir Des Résidus De L'agriculture (Removal of Cationic Dyes by Activated Carbons Synthesized from Agricultural Residues), Thesis, University of Ferhat Abbas Setif-1 Ufas, Algeria, 2014.

[29] N.J. Krou, Etude Expérimentale Et Modélisation D'un Procédé Séquentiel AD-OX D'élimination De Polluants Organiques (Experimental and Modeling Study of a Sequential AD-OX Process for the Removal of Organic Pollutants), Thesis, National polytechnic institute, Toulouse-France, 2010.

[30] L. Sun, F. Meunier, N. Brodu, M.H. Manero, Adsorption: Aspects Théoriques (Adsorption - Theoretical Aspects), France, 2003. https://www.techniques-ingenieur.fr/base-documentaire/archives-th12/archives-operations-unitaires-genie-de-la-reaction-chimique-tiajb/archive-1/adsorption-j2730/.

[31] J. Payaa, J. Monzo, M.V. Borrachero, E.P. Mora, F. Amahjour, Mechanical treatment of fly ashes Part IV. Strength development of ground fly ash-cement mortars cured at different temperatures, Cement Concr. Res. 30 (4) (2000) 543–551, https://doi.org/10.1016/S0008-8846(00)00218-0.

[32] C.S. Poon, L. Lam, Y.L. Wong, A study on high strength concrete prepared with large volumes of low calcium fly ash, Cement Concr. Res. 30 (3) (2000) 447–455, https://doi.org/10.1016/S0008-8846(99)00271-9.

[33] J. Graindorge, E. Landot, La Qualité De L'eau Potable, Techniques Et Responsabilités (Drinking Water Quality, Techniques and Responsibilities), Territorial Editions, 2007.

[34] S. Elabbas, N. Adjeroud, L. Mandi, F. Berrekhis, M.N. Pons, J.P. Leclerc, N. Ouazzani, Eggsell adsorption process coupled with electrocoagulation for improvement of chromium removal from tanning wastewater, Int. J. Environ. Anal.Chem. (2020) 1–13, https://doi.org/10.1080/03067319.2020.1761963.

[35] S.L. Ching, S.Y. Mohd, A.A. Hamidi, M. Umar, Influence of impregnation ratio on coffee ground activated carbon as landfill leachate adsorbent for removal of total iron and orthophosphate, Desalination 279 (2011) 225–234, https://doi.org/10.1016/j.desal.2011.06.011.

[36] B.H. Hameed, Spent tea leaves: a new non-conventional and low-cost adsorbent for removal of basic dye from aqueous solutions, J. Hazard Mater. 161 (2009) 753–759, https://doi.org/10.1016/j.jhazmat.2008.04.019.

[37] K. Malwade, D. Lataye, D. Ramirez, S. Kurwadkar, et al., Adsorption of hexavalent chromium onto activated carbon derived from leucaena leucocephala waste sawdust: kinetics, equilibrium and thermodynamics, Int. J. Environ. Sci. Tech. 13 (9) (2016) 2107–2116, https://doi.org/10.1007/S13762-016-1042-Z.

[38] B.K. Nandi, A. Goswami, M.K. Purkait, Adsorption characteristics of brilliant green dye on kaolin, J. Hazard Mater. 161 (2009) 387–395, https://doi.org/10.1016/j.jhazmat.2008.03.110.

[39] P.T. Dhorabe, D.H. Lataye, R.S. Ingole, Removal of 4-nitrophenol from aqueous solution by adsorption onto activated carbon prepared from Acacia glauca sawdust, Water Sci. Technol. J. 73 (4) (2016) 955–966, https://doi.org/10.2166/Wst.2015.575.

[40] A.A. Attia, S.A. Khedr, S.A. Elkholy, Adsorption of chromium ion (VI) by acid activated carbon. Thermodynamics and Separation Processes Braz, J. Chem. Eng. 27 (1) (2010), https://doi.org/10.1590/S0104-66322010000100016.

[41] D. Tamirat, S. Khalid, A.K. Shimeles, Adsorption of hexavalent chromium from aqueous solution using chemically activated carbon prepared from locally available waste of bamboo (*Oxytenanthera abyssinica*), Int. Sch. Res. Notices (2014), https://doi.org/10.1155/2014/43824.

[42] S. Alvarez-Torrellas, M. Muñoz, J.A. Zazo, J.A. Casas, J. García, Synthesis of high surface area carbon adsorbents prepared from pine sawdust-Onopordum acanthium L. For nonsteroidal anti-inflammatory drugs adsorption, J. Environ. Manag. 183 (2016) 294–305, https://doi.org/10.1016/J.Jenvman.2016.08.077.

[43] P.K. Malik, Dye removal from wastewater using activated carbon developed from sawdust: adsorption equilibrium and kinetics, J. Hazard Mater. 113 (1–3) (2004) 81–88, https://doi.org/10.1016/J.Jhazmat.2004.05.022.

[44] M. Saheed, J.O. Tijani, M.M. Ndamitso, A.A. Saka, A.O. Ajala, M. Abdulkabir, O.J. Oke, Fabrication of porous ceramic pot filters for adsorptive removal of polluants in tannery wastewater, Sci. Afr 11 (2021), e00705, https://doi.org/10.1016/j.sciaf.2021.e00705.

[45] M.A. Renu, K. Singh, Heavy metal removal from wastewater using various adsorbents: a review, J. Water Reuse Desalination 7 (4) (2017) 387–419, https://doi.org/10.2166/wrd.2016.104.

[46] P.S. Blanes, M.E. Bordoni, J.C. Gonzalez, S.I. García, A.M. Atria, L.F. Sala, S.E. Bellú, Application of soy hull biomass in removal of Cr ions from contaminated waters. Kinetic, thermodynamic and continuous sorption studies, J. Environ. Chem. Eng. 4 (1) (2016) 516–526, https://doi.org/10.1016/j.jece.2015.12.008.

[47] C.H. Giles, T. MacEwan, S.N. Nakhwa, D. Smith, Studies in adsorption. Part XI. A system of classification of solution adsorption isotherms, and its use in diagnosis of adsorption mechanisms and in measurement of specific surface areas of solids, J. Chem. Soc. 846 (1960) 3973–3993, https://doi.org/10.1039/Jr9600003973.

[48] N. Yahiaoui, Etude De L'adsorption Des Composés Phénoliques Des Margines D'olives Sur Carbonate De Calcium, Hydroxyhapatite Et Charbon Actif (Adsorption Study of Phenolic Compounds from Oil Mill into Calcium Carbonate, Hydroxyhapatite and Activated Carbon), Thesis at Mouloud Mammeri University, Algeria, 2012.

[49] Osciz (Ed.), Adsorption, Ellis Horwood Limited, John Whiley And Sons, 1982.

[50] S. Bouzid, Adsorption Des Différents Polluants Sur Des Argiles (Adsorption of Different Pollutants into Clays, Thesis at Sciences and Technologies University of Oran, Algeria, 2010.

[51] R. Baccar, Removal of Water Pollutants by Adsorption on Activated Carbon Prepared from Olive- Waste Cakes and by Biological Treatment Using Ligninolytic Fungi, Thesis, University of Barcelone, Spain, 2013.

[52] K.R. Hall, L.C. Eagleton, A. Acrivos, T. Vermeulon, Pore and solid diffusion kinetics in fixed-bed adsorption under constant-pattern conditions, Ing. Eng. Chem. Fundam. 5 (1966) 212–223, https://doi.org/10.1021/i160018a011.

[53] S. Dawood, T.S. Sen, Removal of anionicdye Congo red from aqueus solution by raw pine and acid- treated pine cone powder as adsorbent: equilibrium, thermodynamic , kinetics, mechanism and process design, Water Res. 46 (2012) 1933–1946, https://doi.org/10.1016/j.watres.2012.01.009.

[54] A. Aziz, M.S. Ouali, E. El Hadj, L.C.H. De Menorval, M. Lindheimer, Chemically modified olive stone: a low-cost sorbent for heavy metals and basic dyes removal from aqueous solutions, J. Hazard Mater. 163 (2009) 441–447, https://doi.org/10.1016/j.jhazmat.2008.06.117.

[55] A.A. Ruhan, A. Sabri, M. Tuzen, Equilibrium, thermodynamic and kinetic studies on biosorption of Pb(ii) and Cd (ii) from aqueous solution by macrofungus (*lactarius scrobiculatus*) biomass, Chem. Eng. J. 15 (2009) 255–261, https://doi.org/10.1016/j.cej.2009.03.002.

[56] J. Li, E.B. Carlson, A.A. Lacis, A study on the temporal and spatial variability of absorbing aerosols using total ozone mapping spectrometer and ozone monitoring instrument aerosol index data, J. Geophys. Res. Atmos. 114 (2009) 2156–2202, https://doi.org/10.1029/2008JD011278.